American Mineralogist, Volume 93, pages 1823–1828, 2008

Compression of single-crystal magnesium oxide to 118 GPa and a ruby pressure gauge for helium pressure media

Steven D. Jacobsen,[1,*] Christopher M. Holl,[1] Kimberly A. Adams,[1] Rebecca A. Fischer,[1] Emily S. Martin,[1] Craig R. Bina,[1] Jung-Fu Lin,[2] Vitali B. Prakapenka,[3] Atsushi Kubo,[3] and Przemyslaw Dera[3]

[1]Department of Earth and Planetary Sciences, Northwestern University, Evanston, Illinois 60208, U.S.A.
[2]Department of Geological Sciences, Jackson School of Geosciences, University of Texas, Austin, Texas 78712, U.S.A.
[3]Center for Advanced Radiation Sources, University of Chicago, Chicago, Illinois 60637, U.S.A.

Abstract

The pressure-volume equation of state (EoS) of single-crystal MgO has been studied in diamond-anvil cells loaded with helium to 118 GPa and in a non-hydrostatic KCl pressure medium to 87 GPa using monochromatic synchrotron X-ray diffraction. A third-order Birch-Murnaghan fit to the non-hydrostatic *P-V* data (KCl medium) yields typical results for the initial volume, V_0 = 74.698(7) Å^3, bulk modulus, K_{T0} = 164(1) GPa, and pressure derivative, K' = 4.05(4), using the non-hydrostatic ruby pressure gauge of Mao et al. (1978). However, compression of MgO in helium yields V_0 = 74.697(6) Å^3, K_{T0} = 159.6(6) GPa, and K' = 3.74(3) using the quasi-hydrostatic ruby gauge of Mao et al. (1986). In helium, the fitted equation of state of MgO underdetermines the pressure by 8% at 100 GPa when compared with the primary MgO pressure scale of Zha et al. (2000), with K_{T0} = 160.2 GPa and K' = 4.03. The results suggest that either the compression mechanism of MgO changes above 40 GPa (in helium), or the ruby pressure gauge requires adjustment for the softer helium pressure medium. We propose a ruby pressure gauge for helium based on shift of the ruby-R_1 fluorescence line ($\Delta\lambda/\lambda_0$) and the primary MgO pressure scale, with P (GPa) = $A/B\{[1 + (\Delta\lambda/\lambda_0)]^B - 1\}$, where A is fixed to 1904 GPa and B = 10.32(7).

Keywords: MgO, helium pressure medium, static compression, equation of state, ruby fluorescence

Introduction

Magnesium oxide (MgO, periclase) is among the most widely studied standard materials for testing experimental and theoretical methods of determining elastic properties (Spetzler 1970; Jackson and Niesler 1982; Chang and Cohen 1984; Isaak et al. 1989; Chen et al. 1998; Duffy and Ahrens 1995; Karki et al. 1999; Sinogeikin and Bass 2000; Zha et al. 2000; Speziale et al. 2001; Jacobsen et al. 2002). MgO maintains the *B*1 (halite) structure to multi-megabar pressures (Duffy et al. 1995) and is geophysically important as end-member ferropericlase, (Mg,Fe)O, thought to be the major non-silicate oxide of the lower mantle. Because of its simple structure and geophysical relevance, knowledge of accurate elastic properties of MgO pertains to problems ranging from experimental pressure scales to interpreting Earth's seismic structure.

Recent discoveries in mineral physics of the lower mantle, especially electronic spin transitions of iron (Badro et al. 2003; Lin et al. 2007) and the post-perovskite phase of $MgSiO_3$ (Murakami et al. 2004; Oganov and Ono 2004), present the need for reliable pressure scales in the 25–140 GPa range. In the deep mantle, conditions of stress are essentially hydrostatic. Such conditions of uniform stress are difficult to achieve in diamond cells because no known element or compound remains fluid above 10–15 GPa at 300 K (Angel et al. 2007). Although argon and neon are commonly used as "quasi-hydrostatic" pressure-transmitting media in diamond cells, helium is preferred because it applies near-hydrostatic stress to at least 50 GPa (Takemura 2001; Dewaele and Loubeyre 2007), preserving the quality of delicate single-crystal plates ≤10 μm in thickness for high-pressure crystallographic studies at lower-mantle pressures.

Previous static-compression studies of MgO using helium as the pressure medium reached 55 GPa (Zha et al. 2000) and 52 GPa (Speziale et al. 2001), both employing energy dispersive synchrotron X-ray diffraction from polycrystalline samples. Here we extend *P-V* measurements of MgO to 118 GPa on single crystals in helium using angle-dispersive, monochromatic synchrotron X-ray diffraction. The extended pressure range improves analysis of the pressure derivative of the bulk modulus (K') from Birch-Murnaghan equations of state. Using pressures from the quasi-hydrostatic ruby scale of Mao et al. (1986), the fitted EoS for MgO compressed in helium exhibits unusually low values of K' = 3.7. Deviation of K' from typical ultrasonic and Brillouin scattering values of 4.0–4.1 (Jackson and Niesler 1982; Sinogeikin and Bass 2000) and the primary MgO pressure scale with K' = 4.03 (Zha et al. 2000) accounts for about 8–10 GPa pressure difference (ΔP) in the 100–120 GPa pressure range. Because an upwards adjustment in pressure was required in going from the non-hydrostatic ruby-pressure gauge (Mao et al. 1978) to the so-called quasi-hydrostatic pressure gauge (Mao et al. 1986) calibrated in an argon medium, a similar adjustment for the softer helium medium can account for the anomalously

* E-mail: steven@earth.northwestern.edu

low K' reported here for MgO, as well as the anomalously low $K' = 3.0(1)$ reported for single-crystal diamond compressed in helium to 140 GPa (Occelli et al. 2003). Several recent studies have proposed such adjustment in ruby-fluorescence pressures for helium media using various equations of state of metals (Dewaele et al. 2004; Chijioke et al. 2005; Silvera et al. 2007). Here we calibrate the ruby-pressure gauge for helium against the primary MgO pressure scale of Zha et al. (2000). The new pressure gauge will be useful for future high-pressure crystallographic studies of minerals compressed with helium in the 25–140 GPa range of the lower mantle.

Experimental methods

Magnesium oxide [100]-substrates with >99.95% purity were obtained commercially from MTI Corporation. Diamond lapping film was used to polish the MgO to 5–8 μm thickness. Cleavage fragments measuring approximately 10 × 10 μm were prepared for loading into diamond-anvil cells. We used symmetric-piston diamond cells, fitted with beveled diamond anvils having 100 μm inner culets and 300 μm outer culets. Rhenium gaskets were pre-indented to 26–28 GPa, resulting in about 25 μm initial gasket thickness. An electrostatic discharge machine was used to erode symmetric holes approximately 80 μm diameter in the Re gaskets, just smaller than the 100 μm inner culet. The diamond cells were also fitted with cubic boron nitride (cBN) seats, placed downstream of the synchrotron source to allow wide angular access to diffracted X-rays, while tungsten carbide seats were used on the upstream side. The cBN seats allowed oscillation of cells about the vertical axis by ±10°, without producing diffraction from the parts of the diamond cell (Fig. 1).

Diamond cells were loaded using the COMPRES/GSECARS gas-loading system at sector 13 of the Advanced Photon Source (Rivers et al. 2008). Helium was compressed at ~160 MPa into the diamond cells, which were closed with a piston to about 4–6 GPa under in situ video monitoring and ruby fluorescence. At this initial loading pressure, gasket-hole diameters had reduced by 40% to about 50 μm diameter. Annealed ruby spheres were used as pressure markers. Three separate helium runs were carried out on the 13-BMD beamline of GSECARS, labeled runs 1, 2, and 3 in the tables and figures. In the present analysis, data from all three helium runs have been merged into a single data set (Table 1). In a separate diamond cell with 200 μm flat culets, an MgO crystal and ruby pressure markers were loaded with a KCl pressure medium (Table 2). In all runs, X-ray diffraction patterns were recorded on a MAR-345 image plate using monochromatic synchrotron radiation at 45 keV (λ = 0.27552 Å). Representative diffraction patterns from the helium and KCl runs are shown in Figure 1.

Results and discussion

Up to eight reflections of the *hk*0 class were indexed (Fig. 1) and used in least-squares cell refinement with "UnitCell," a non-linear regression routine by Holland and Redfern (1997). For initial analysis of EoS parameters, unit-cell volumes from helium runs 1–3 are listed in Table 1, along with pressures determined from the quasi-hydrostatic pressure scale of Mao et al. (1986). The ruby fluorescence signal was lost in the six highest pressures of run 3, where we relied on the diamond-Raman shift using Equation 4a of Sun et al. (2005), calibrated against the ruby scale of Mao et al. (1986). The diamond-Raman pressures were weighted less in the EoS fitting by assuming a relatively large

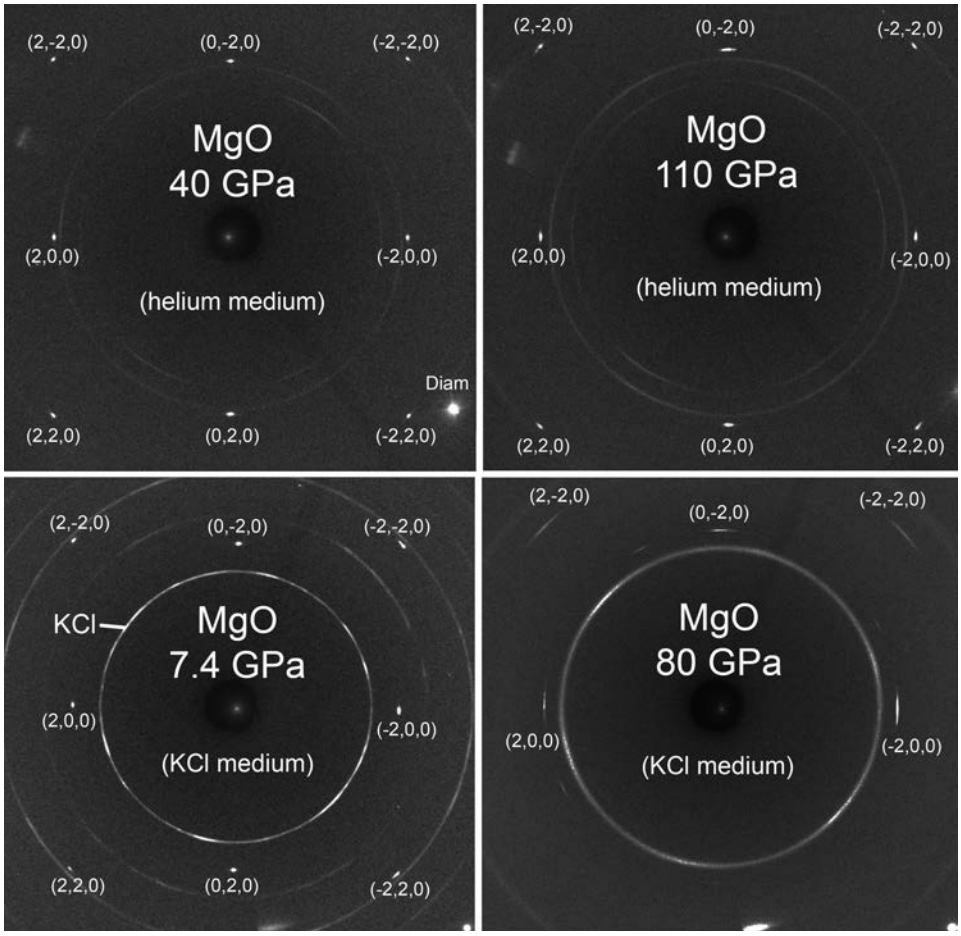

Figure 1. [100]-zone diffraction patterns of single-crystal MgO compressed in a helium pressure medium at 40 and 110 GPa (upper panels) and in a KCl pressure medium at 7.4 and 80 GPa (lower panels) taken with monochromatic synchrotron radiation at 45 keV. Diffraction patterns are rotated to place the (2,0,0) diffraction spots on the horizontal axis.

TABLE 1. X-ray diffraction data for single-crystal MgO compressed in helium

Run	Ruby R_1 shift ($\Delta\lambda/\lambda_0$)	Ruby-scale *P* (GPa)*	Volume (Å^3)	MgO-scale *P* (GPa)†
		0.0001	74.698(3)‡	
1	0.00439	8.5(1)	71.184(37)	8.5
1	0.00626	12.2(2)	69.812(36)	12.4
1	0.00781	15.3(2)	68.759(33)	15.7
1	0.00929	18.2(1)	67.911(32)	18.5
1	0.01182	23.4(1)	66.483(31)	23.6
1	0.01407	28.1(1)	65.279(33)	28.3
1	0.01495	29.9(1)	64.813(32)	30.3
1	0.01712	34.5(1)	63.631(37)	35.5
1	0.01858	37.6(1)	62.882(37)	39.1
1	0.01983	40.4(1)	62.287(36)	42.0
1	0.02100	42.9(1)	61.744(30)	44.8
1	0.02281	46.9(1)	61.029(30)	48.7
1	0.02409	49.7(1)	60.426(29)	52.1
1	0.02556	53.0(1)	59.931(29)	55.1
1	0.02694	56.1(1)	59.430(29)	58.1
1	0.02841	59.5(1)	58.867(28)	61.7
1	0.02984	62.8(1)	58.335(28)	65.3
1	0.03103	65.6(2)	57.918(28)	68.2
1	0.03220	68.3(2)	57.480(27)	71.3
2	0.00340	6.5(1)	71.896(7)	6.6
2	0.00436	8.4(1)	71.169(7)	8.6
2	0.00591	11.5(1)	70.070(6)	11.7
2	0.00683	13.3(1)	69.472(6)	13.5
2	0.00948	18.6(2)	67.798(6)	18.9
2	0.01144	22.6(2)	66.655(7)	23.0
2	0.01374	27.4(1)	65.404(6)	27.8
3	0.00228	4.3(1)	72.788(7)	4.4
3	0.00413	7.9(1)	71.229(7)	8.4
3	0.00598	11.6(1)	69.907(6)	12.1
3	0.00907	17.8(1)	67.977(7)	18.3
3	0.01207	23.9(1)	66.270(6)	24.4
3	0.01529	30.6(1)	64.535(6)	31.5
3	0.01804	36.5(1)	63.176(6)	37.6
3	0.01974	40.1(1)	62.412(5)	41.4
3	0.02140	43.7(1)	61.548(5)	45.9
3	0.02277	46.8(1)	61.031(5)	48.7
3	0.02469	51.0(1)	60.252(5)	53.2
3	0.02660	55.3(3)	59.593(5)	57.1
3	0.02795	58.4(3)	59.084(5)	60.3
3	0.02990	62.9(1)	58.339(7)	65.3
3	0.03146	66.5(1)	57.744(5)	69.4
3	0.03275	69.6(2)	57.271(5)	72.8
3	0.03487	74.6(4)	56.471(5)	78.9
3	0.03712	80.0(13)	55.834(5)	84.0
3	0.03955	85.0(1)	55.110(5)	90.1
3		89.0(20)§	54.628(5)	94.4
3		96.2(20)§	53.719(4)	102.9
3		99.6(20)§	53.361(4)	106.4
3		102.4(20)§	53.067(4)	109.4
3		106.3(20)§	52.639(4)	113.8
3		111.0(20)§	52.239(4)	118.1

Note: Standard deviations in the last digits are shown in parentheses.
* Ruby-scale pressures from Mao et al. (1986) with standard deviation of 0.1 GPa, unless the pressure difference before and after volume measurement is greater, as reported.
† Calculated pressure from the primary MgO scale of Zha et al. (2000).
‡ Experimental V_0 from single-crystal X-ray diffraction data of Jacobsen et al. (2002).
§ Pressures from diamond-Raman shift, Sun et al. (2005), assumed uncertainty is ±2.0 GPa.

TABLE 2. X-ray diffraction data for single-crystal MgO compressed in a KCl pressure medium

Ruby-scale *P* (GPa)*	Volume (Å^3)
3.6(1)	73.100(7)
7.4(1)	71.791(7)
10.6(1)	70.606(6)
13.5(1)	69.620(6)
16.2(1)	68.695(7)
18.9(1)	67.858(7)
22.8(1)	66.847(7)
26.9(1)	65.785(6)
31.1(1)	64.735(6)
36.6(6)	63.546(6)
41.4(4)	62.573(7)
49.1(1)	61.258(7)
52.2(2)	60.709(6)
53.5(4)	60.493(6)
55.9(8)	60.062(6)
58.1(1)	59.617(7)
61.1(1)	59.257(7)
63.5(2)	58.830(7)
65.9(1)	58.485(7)
68.7(2)	58.247(6)
71.2(2)	57.737(6)
73.9(3)	57.335(6)
76.2(3)	57.116(6)
80.1(1)	56.609(6)
83.5(3)	56.107(6)
86.6(1)	55.792(6)

* Non-hydrostatic ruby-scale pressures from Mao et al. (1978).

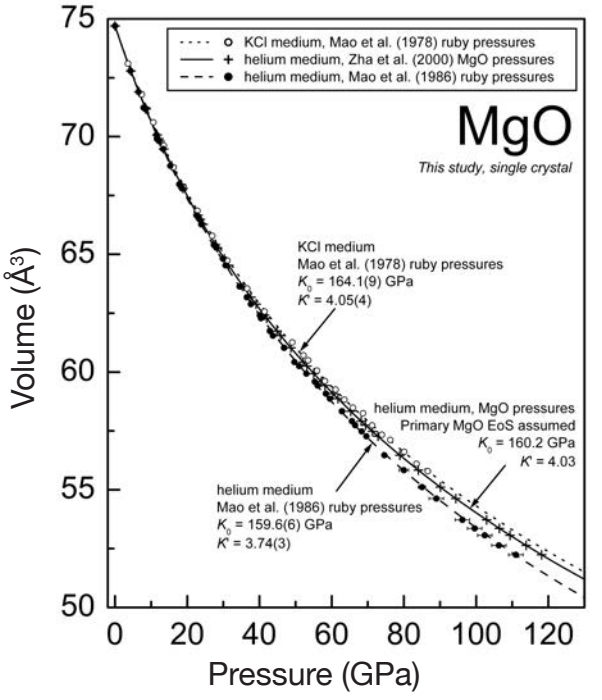

FIGURE 2. Volume-compression data of single-crystal MgO in a non-hydrostatic KCl pressure medium (open circles) and in helium (filled circles). The dashed curve is the fitted EoS using the ruby gauge of Mao et al. (1986). The solid curve shows the primary MgO equation of state from Zha et al. (2000).

uncertainty of ±2 GPa. Volumes from the non-hydrostatic run in KCl are provided in Table 2, with ruby pressures calculated from the non-hydrostatic ruby gauge of Mao et al. (1978).

Volume-compression data from the three helium runs and one non-hydrostatic run (KCl medium) are plotted together in Figure 2. Using the experimental initial volume $V_0 = 74.698(3)$ Å^3 of Jacobsen et al. (2002) and fitting a third-order Birch-Murnaghan equation of state to the non-hydrostatic data (KCl medium) yields $V_0 = 74.698(7)$ Å^3, $K_{T0} = 164.1(9)$ GPa, and $K' = 4.05(4)$. When the V_0 point is excluded from the fitting, we obtain $V_0 = 74.73(8)$ Å^3, $K_{T0} = 163(2)$ GPa, and $K' = 4.08(7)$. If K' is fixed to 4.03 after Zha et al. (2000), we obtain $V_0 = 74.69(4)$ Å^3 and $K_{T0} = 164.6(7)$ GPa. Because exclusion of experimental V_0 or fixing K' does not

influence the fitted parameters beyond one standard deviation, the preferred three-parameter fit to the non-hydrostatic data are shown in Figure 2 by the dotted curve.

A three-parameter fit to the helium-medium data from all three runs (Table 1) yields $V_0 = 74.687(6)$ Å^3, $K_{T0} = 159.6(6)$, and $K' = 3.74(3)$, plotted as the dashed curve in Figure 2. Excluding the six highest pressures of run 3, which were determined from the diamond-Raman shift (Sun et al. 2005), yields the same EoS parameters within uncertainty: $V_0 = 74.697(7)$ Å^3, $K_{T0} = 159.5(6)$ GPa, and $K' = 3.74(3)$ (using ruby pressures only). For comparison with Speziale et al. (2001), who fixed $K_{T0} = 160.2$ GPa, we obtain $V_0 = 74.695(6)$ GPa and $K' = 3.709(8)$ with fixed $K_{T0} = 160.2$ GPa. The resulting K' is significantly lower than the reported Speziale et al. (2001) value of $K' = 3.99(1)$, however, when the Speziale et al. (2001) data set is fitted with three parameters, they obtain $V_0 = 74.53(2)$ Å^3, $K_{T0} = 170(1)$ GPa, with $K' = 3.59$. To further analyze the current results in comparison with the helium-only data of Speziale et al. (2001) and the primary MgO pressure scale (Zha et al. 2000), all the data are plotted in Figure 3 as normalized pressure (F) against Eulerian strain (f), where $F = P/3f(1+2f)^{5/2}$ and $f = [(V_0/V)^{2/3} - 1]/2$. The F-f plot is a convenient way of viewing the compression data because the third-order Birch-Murnaghan EoS can be drawn as a straight line with slope $3K_0(K' - 4)/2$ and intercept of K_0.

Non-hydrostatic (KCl medium) compression data of MgO are plotted as open circles in Figure 3 and fitted EoS shown as a dotted line with $K' = 4.05(4)$. In contrast, helium-medium data (filled circles in Fig. 3) exhibit $K' < 4$, shown by the dashed line with $K' = 3.74(3)$. To demonstrate the reproducibility of this observation, we shaded runs 1 and 3 differently in Figure 3, showing that both runs are consistent with $K' < 4$. Furthermore, if the helium-only data of Speziale et al. (2001) are re-analyzed with a third-order Birch-Murnagahn EoS we obtain $K_{T0} = 165(1)$ GPa and $K' = 3.74(7)$, shown by the filled triangles and dash-dotted line in Figure 3. Thus, three separate helium-medium datasets produce $K' = 3.74$, namely runs 1 and 3 of the current study, and Speziale et al. (2001), helium subset.

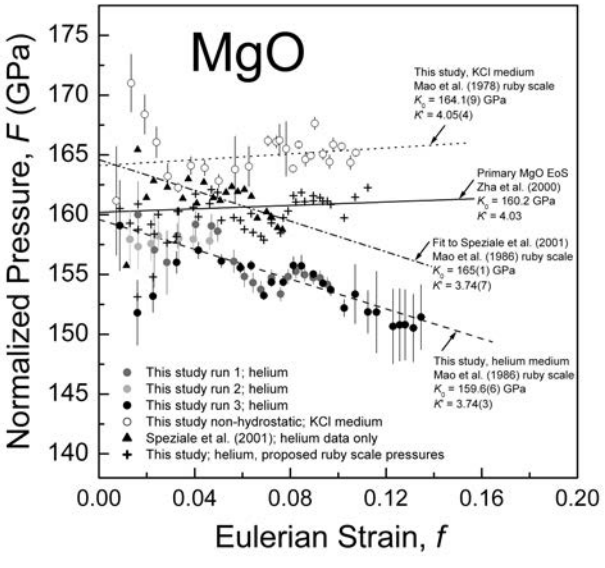

FIGURE 3. *F-f* plot for MgO compression data based on the third-order Birch-Murnaghan equation of state. The non-hydrostatic run in KCl is shown by open circles. Current runs 1–3 using helium media are shown by filled circles, and the helium-media data of Speziale et al. (2001) are shown by filled triangles. All helium-media data sets using ruby pressures of Mao et al. (1986) give $K' = 3.74$, which underestimate the pressure by 8–10% at 100–120 GPa compared with the primary MgO scale (solid line, Zha et al. 2000).

Because the current measurements were conducted on single-crystal samples using angle-dispersive diffraction compared with polycrystalline samples and energy dispersive techniques (Zha et al. 2000; Speziale et al. 2001), we consider the possible magnitude of deviatoric stress on measured lattice parameters. Dewaele and Loubeyre (2007) estimated differences in the stress component along the diamond-cell loading axis compared with stress in the plane normal to the loading axis for helium media to be 0.3–0.5 GPa at 150 GPa. Because the estimated deviatoric stress of 0.3 GPa at 100 GPa (Dewaele and Loubeyre 2007) is on the order of the precision of the ruby-pressure determination, we did not make a correction to our lattice parameters for deviatoric stress. We also note that 0.3 GPa is over $25\times < \Delta P$ of ~8 GPa calculated between the quasi-hydrostatic ruby pressures and MgO pressures at 100 GPa. Finally, because we also carried out identical single-crystal and angle-dispersive measurements on MgO in a highly non-hydrostatic (KCl) pressure medium, resulting in $K' = 4.05(4)$, we further scrutinize other possible causes of the anomalously low $K' = 3.74(3)$ obtained for MgO compressed in helium.

Zha et al. (2000) obtained primary pressures up to 55 GPa with MgO because their combined high-pressure X-ray diffraction and Brillouin scattering measurements allowed direct pressure determination without reference to a secondary calibrant. In the current study, the observed deviation of K' from the primary MgO scale with $K' = 4.03$ in helium might be interpreted in several ways. Either K' evolves to lower values (through more negative K'') above 50 GPa by a different compression mechanism, possibly influenced by diffusion of helium into the MgO sample, or the ruby fluorescence scale of Mao et al. (1986) requires adjustment for helium pressure media above about 50 GPa. The shear strength of argon, which was used as the pressure-transmitting medium in the Mao et al. (1986) ruby-gauge calibration, was recently shown to rise dramatically in the 30–50 GPa pressure range (Mao et al. 2006). It is also notable that extrapolation of the Zha et al. (2000) MgO pressures into the 50–100 GPa pressure range is not without uncertainty, however, because K' values of about 4 are consistent with ultrasonic (Jackson and Niesler 1982; Yoneda 1990) and Brillouin scattering studies (Sinogeikin and Bass 2000) in the 0–20 GPa range, as well as with shock-wave (Duffy and Ahrens 1995) and first-principles studies (Karki et al. 1999) in the 50–150 GPa range, we continue with the underlying assumption that K' should be ~4 in the Birch-Murnaghan formulation over the current experimental pressure range. Examination of all the *F-f* data in Figure 3 shows that at strains <~0.06 (pressures below about 40 GPa), the helium data are adequately modeled with $K' \sim 4$. Only five or six of the highest points from Speziale et al. (2001) fall into the range where $K' < 4$. The current data, extending to >100 GPa reveal a clearer trend of decreasing K' with strain. However, the fact

that our non-hydrostatic compression data in KCl, measured in the same way, reproduce typical values for the equation of state of MgO (dotted line in Fig. 3) suggests a closer examination of the quasi-hydrostatic ruby pressure gauge.

A re-calibration to higher pressures was required in going from the non-hydrostatic ruby gauge (Mao et al. 1978) to the so-called quasi-hydrostatic ruby pressure gauge (Mao et al. 1986) calibrated against the EoS of Cu in an argon medium. Diffraction peak-broadening, indicative of non-hydrostatic stress, has been reported in argon media above 1.9 GPa (Angel et al. 2007), in contrast to at least 50 GPa for helium (Takemura 2001). Furthermore, the strength of argon increases rapidly with pressure above 20–30 GPa, exhibiting shear strength >2.7 GPa at 55 GPa (Mao et al. 2006). Because the quasi-hydrostatic ruby pressure gauge was calibrated from experiments using an argon medium, the observed differences between MgO and quasi-hydrostatic ruby pressures documented here could be attributed to dramatic stiffening of the argon medium in the ruby calibration of Mao et al. (1986).

Following the formulation of Mao et al. (1978), ruby pressures are calculated from the measured shift ($\Delta\lambda/\lambda_0$) of the R_1 ruby fluorescence line using P (GPa) = A/B $\{[1 + (\Delta\lambda/\lambda_0)]^B - 1\}$. By fixing A = 1904 GPa, the value of B is 5.0 for the non-hydrostatic scale (Mao et al. 1978) and 7.665 for the quasi-hydrostatic scale (Mao et al. 1986), shown in Figure 4 by the dotted and dashed curves, respectively. Using our single-crystal volume data for MgO and the primary pressure scale of Zha et al. (2000), we obtain a revised ruby calibration for helium with A = 1930(6) GPa and B = 9.44(23) GPa. The corresponding reduced χ^2 is 0.08195 and R^2 = 0.99986 when the A parameter is allowed to refine. In keeping with the formulation of Mao et al. (1986), we fixed A = 1904 GPa and obtained B = 10.32(7) with a χ^2 of 0.1077 and R^2 = 0.99982, shown by the solid curve in Figure 4. We present the current calibration as a secondary pressure gauge for high-pressure studies of minerals using helium pressure media in the lower-mantle pressure range of 23–140 GPa.

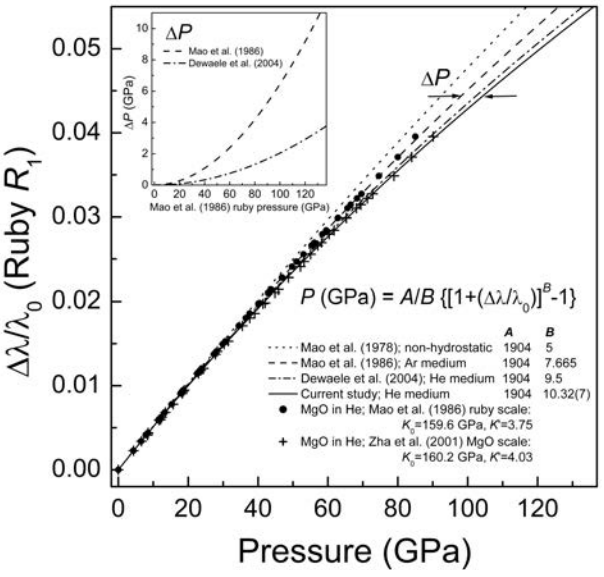

FIGURE 4. Proposed ruby pressure gauge (solid line) based on the shifts of the R_1 ruby fluorescence line ($\Delta\lambda/\lambda_0$) and the primary MgO pressure scale of Zha et al. (2000), compared with the non-hydrostatic ruby gauge (Mao et al. 1978, dotted line) and the helium-medium calibration from various metals (Dewaele et al. 2004, dash-dotted line). Calculated pressure differences are plotted inset.

Re-calibration of the ruby-pressure gauge for helium-loaded diamond cells against MgO pressures is pragmatic following many decades of mineral physics research on this standard material. The combined X-ray diffraction and Brillouin scattering study of Zha et al. (2000) provides direct pressures because the equation of state was obtained without reference any prior pressure standard. Further justification of using MgO to re-calibrate the ruby scale for the effectively quasi-hydrostatic medium, helium, stems from a range of observations indicating that K' should be about 4 in the Birch-Murnaghan equation of state over a wide range of pressures, including ultrasonic interferometry (Jackson and Niesler 1982; Yoneda 1990), Brillouin scattering (Sinogeikin and Bass 2000), shock-wave (Duffy and Ahrens 1995) and first-principles studies (Karki et al. 1999). Future work should include a cross-check of the MgO-based ruby gauge for helium with metals used in similar studies (Dewaele et al. 2004; Chijioke et al. 2005; Silvera et al. 2007), as well as detailed analysis of the possible effects of anisotropic stress fields in polycrystalline vs. single-crystal experiments in the pressure range of the lower mantle.

ACKNOWLEDGMENTS

Work performed at GeoSoilEnviroCARS (Sector 13), Advanced Photon Source (APS), Argonne National Laboratory was supported by the U.S. National Science Foundation (EAR-0622171) and the Department of Energy (DOE), DE-FG02-94ER14466. Use of the Advanced Photon Source was supported by the U.S. DOE, Office of Science, Office of Basic Energy Sciences, under Contract no. DE-AC02-06CH11357. J.F.L. acknowledges support through the auspices of the U.S. DOE by Lawrence Livermore National Laboratory, DE-AC52-07NA27344, and a Lawrence Livermore Fellowship. S.D.J. acknowledges support from the Carnegie/DOE Alliance Center (CDAC) and NSF grant EAR-0721449.

REFERENCES CITED

Angel, R.J., Bujak, M., Zhao, J., Gatta, G.D., and Jacobsen, S.D. (2007) Effective hydrostatic limits of pressure media for high-pressure crystallographic studies. Journal of Applied Crystallography, 40, 26–32.

Badro, J., Fiquet, G., Guyot, F., Rueff, J.P., Struzhkin, V.V., Vankò, G., and Monaco, G. (2003) Iron partitioning in Earth's mantle: Toward a deep lower mantle discontinuity. Science, 300, 789–791.

Chang, K.J. and Cohen, M.L. (1984) High-pressure behavior of MgO: Structural and electronic properties. Physical Review B, 30, 4774–4781.

Chen, G., Liebermann, R.C., and Weidner, D.J. (1998) Elasticity of single-crystal MgO to 8 gigpascals and 1600 Kelvin. Science, 280, 1913–1916.

Chijioke, A.D., Nellis, W.J., Soldatov, A., and Silvera, I.F. (2005) The ruby pressure standard to 150 GPa. Journal of Applied Physics, 98, 114905.

Dewaele, A. and Loubeyre, P. (2007) Pressurizing conditions in helium-pressure-transmitting medium. High-Pressure Research, 27, 419–429.

Dewaele, A., Loubeyre, P., and Mezouar, M. (2004) Equations of state of six metals above 94 GPa. Physical Review B, 70, 094112.

Duffy, T.S. and Ahrens, T.J. (1995) Compressional sound velocity, equation of state, and constitutive response of shock-compressed magnesium oxide. Journal of Geophysical Research, 100, 529–542.

Duffy, T.S., Hemley, R.J., and Mao, H.K. (1995) Equation of state and shear strength at multimegabar pressures: Magnesium oxide to 227 GPa. Physical Review Letters, 74, 1371–1374.

Holland, T.J.B. and Redfern, S.A.T. (1997) Unit cell refinement from powder diffraction data: The use of regression diagnostics. Mineralogical Magazine, 61, 65–77.

Isaak, D.G., Anderson, O.L., and Goto, T. (1989) Measured elastic moduli of single-crystal MgO up to 1800 K. Physics and Chemistry of Minerals, 16, 704–713.

Jackson, I. and Niesler, H. (1982) The elasticity of periclase to 3 GPa and some geophysical implications. In S. Akimoto and M.H. Manghnani, Eds., High

Pressure Research in Geophysics, p. 93–113. Center for Academic Publishing, Tokyo, Japan.
Jacobsen, S.D., Reichmann, H.J., Spetzler, H.A., Mackwell, S.J., Smyth, J.R., Angel, R.J., and McCammon, C.A. (2002) Structure and elasticity of (Mg,Fe)O and a new method of generating shear waves for gigahertz ultrasonic interferometry. Journal of Geophysical Research, 197, 2037.
Karki, B.B., Wentzcovitch, R.M., de Gironcoli, S., and Baroni, S. (1999) First-principles determination of elastic anisotropy and wave velocities of MgO at lower mantle conditions. Science, 286, 1705–1707.
Lin, J.F., Vankó, G., Jacobsen, S.D., Iota, V., Struzhkin, V.V., Prakapenka, V.B., Kuznetsov, A., and Yoo, C.S. (2007) Spin transition zone in Earth's lower mantle. Science, 317, 1740–1743.
Mao, H.K., Bell, P.M., Shaner, J., and Steinberg, D. (1978) Specific volume measurements of Cu, Mo, Pd, and Ag and calibration of the ruby R_1 fluorescence pressure gauge from 0.06 to 1 Mbar. Journal of Applied Physics, 49, 3276–3283.
Mao, H.K., Xu, J., and Bell, P.M. (1986) Calibration of the ruby pressure gauge to 800 kbar under quasi-hydrostatic conditions. Journal of Geophysical Research, 91, 4673–4676.
Mao, H.K., Badro, J., Shu, J., Hemley, R.J., and Singh, A.K. (2006) Strength, anisotropy, and preferred orientation of solid argon at high pressures. Journal of Physics: Condensed Matter, 18, S963–S968.
Murakami, M., Hirose, K., Kawamura, K., Sata, N., and Ohishi, Y. (2004) Post-perovskite transition in $MgSiO_3$. Science, 304, 855–858.
Occelli, F., Loubeyre, P., and Letoullec, R. (2003) Properties of diamond under hydrostatic pressures up to 140 GPa. Nature Materials, 2, 151–154.
Oganov, A.R. and Ono, S. (2004) Theoretical and experimental evidence for a post-perovskite phase of $MgSiO_3$ in Earth's D″ layer. Nature, 430, 445–448.
Rivers, M., Prakapenka, V.B., Kubo, A., Pullins, C., Holl, C.M., and Jacobsen, S.D. (2008) The COMPRES/GSECARS gas loading system for diamond anvil cells at the Advanced Photon Source. High-Pressure Research, 28, in press, DOI: 10.1080/08957950802333593.
Sinogeikin, S.V. and Bass, J.D. (2000). Single-crystal elasticity of pyrope and MgO to 20 GPa by Brillouin scattering in the diamond cell. Physics of the Earth and Planetary Interiors, 120, 43–62.
Spetzler, H. (1970) Equation of state of polycrystalline and single crystal MgO to 8 kilobars and 800°K. Journal of Geophysical Research, 75, 2073–2087.
Speziale, S., Zha, C.-S., Duffy, T.S., Hemley, R.J., and Mao, H.K. (2001) Quasi-hydrostatic compression of magnesium oxide to 52 GPa: Implications for the pressure-volume-temperature equation of state. Journal of Geophysical Research, 106, 515–528.
Sun, L., Ruoff, A.L., and Stupian, G. (2005) Convenient pressure gauge for multimegabar pressures calibrated to 300 GPa. Applied Physics Letters, 86, 014103.
Silvera, I.F., Chijioke, A.D., Nellis, W.J., Soldatov, A., and Tempere, J. (2007) Calibration of the ruby pressure scale to 150 GPa. Physica Status Solidi, 244, 460–467.
Takemura, K. (2001) Evaluation of the hydrostaticity of a helium-pressure medium with powder X-ray diffraction techniques. Journal of Applied Physics, 89, 662–668.
Yoneda, A. (1990) Pressure derivatives of elastic constants of single crystal MgO and $MgAl_2O_4$. Journal of Physics of the Earth, 38, 19–55.
Zha, C.-S., Mao, H.K., and Hemley, R.J. (2000) Elasticity of MgO and a primary pressure scale to 55 GPa. Proceedings of the National Academy of Sciences U.S.A., 97, 13494–13499.

Manuscript received March 26, 2008
Manuscript accepted May 15, 2008
Manuscript handled by Bryan Chakoumakos